Földtani Közlöny 137/4, 581–598. (2007) Budapest

X-ray computer tomography in clastic sedimentology

Röntgen komputer tomográf alkalmazása a törmelékes szedimentológiában

Zoltán HUNYADFALVI[1]

(16 figures)

Keywords: clastic sediments, X-ray attenuation, numeric analysis, texture, grain size, autocorrelogram, spatial continuity, small-scale static flow

Tárgyszavak: törmelékes üledékek, röntgen sugárgyengítés, numerikus vizsgálat, szövet, szemcseméret, autokorrelogram, térbeli folytonosság, kisléptékű statikus áramlások

Összefoglalás

A különböző felhalmozódási környezetek változatos üledékes fáciesből épülnek fel, képviselve a változatos fizikai, kémiai, és biológiai folyamatokat, amelyek jellegzetes törmelékes üledékes szövet típusokat (texture/fabric) alakítanak ki. A törmelékes üledékes kőzetek sugárgyengítése általában a térfogati sűrűségtől, az atomszámtól, a pórusok fluidumtartalmától, a szemcsék, a cement, valamint a lehetséges póruskitöltő fluidum kémiai összetételétől függ. A szöveti tulajdonságok közül, a szemcseméret az egyik legfontosabb, amely hatással van mind a térfogati sűrűségre, mind a sugárgyengítésre. Az orvosi CT felbontása alkalmas a 0,1 milliméteres tartomány feletti szemcseméret változásából adódó sugárgyengítési érték megváltozásának észlelésére. A törmelékes üledékes kőzetek numerikus azonosíthatósága azon a megfigyelésen alapszik, hogy minden szövettípus jellemezhető egy Hounsfield egység intervallummal, figyelembe véve annak korát, és felhalmozódásának jellegét. Az intervallumok között átlapolódások jöhetnek létre. Ennek elkerülésére, normális eloszlású adatsor esetében, a várható érték, míg nem normális adatsor esetében a medián, vagy a 'maximum-likelihood' módszerrel becsült középérték használandó. Az autokorreláció, vagy pontosabban az autokorrelogram alkalmas a síkbeli folytonosság térbeli elemzésére. A legalább gyenge stacionaritással bíró regionalizált változó félvariogramja és annak síkbeli autokorrelációja között fennálló függvénykapcsolat, lehetővé teszi, hogy az autokorrelogram felszínét, mint az eredeti adatok térbeli folytonosságának képét alkalmazzuk. Így a síkbeli autokorrelogram a mérési adatok teljes statisztikai rendszerét adja meg. A Laplace-operátor egy olyan matematikai eszköz, amellyel egy adott pontban a fizikai mennyiségek nettó hozzá-, illetve eláramlását tudjuk meghatározni. A Laplace-operátor alkalmazásával előállított gridek, jó egyezést mutatnak a törmelékes üledékes kőzetek szerkezeti és heterogenitási tulajdonságaival. Ebből következően, a módszer alkalmazható potenciális áramlási pályák kijelölésére. A magfeltöltéses vizsgálatokban való alkalmazása elősegíti a rezervoár kőzetekben, mikro-léptékben lezajló fluidáramlások jobb megértését, és előre jelezhetőségét. A dolgozatnak két fő célja van: első, hogy bemutassa, a CT mérésekből származó adatok elemzésével az alapvető törmelékes üledékes kőzetek numerikusan azonosíthatóak és megkülönböztethetőek egymástól; másodszor, hogy a Laplace- operátor alkalmazásával előállított gridek jó egyezést mutatnak a törmelékes üledékes kőzetek szerkezeti és heterogenitási tulajdonságaival, valamint, hogy ennek a módszernek az alkalmazásával, az orvosi CT felbontási tartományában lehetőség van potenciális áramlási pályák kijelölésére.

Abstract

Depositional environments composed of diverse sedimentary facies that represent the variability of different physical, chemical and biological conditions which generate characteristic textures and fabrics of clastic sedimentary rocks. X-ray attenuation of clastic sedimentary rocks generally depends on bulk density, effective atomic number, fluid content, and the chemical composition of grains, cement and fluid

[1]Department of Geology and Paleontology, University of Szeged, 6701 Szeged P. O. Box: 658;
zoli@geo.u-szeged.hu

content if present. Grain size is one of the most important characteristics of texture which affects bulk density and consequently X-ray attenuation. The resolution of medical CT is suitable for detecting the changes in X-ray attenuation which originate in grain size alteration above 0.1 mm. Numerical identification of clastic sedimentary rocks, based on the observation that every type of texture could be represented by different intervals of Hounsfield Units (HUs), takes age and depositional history into consideration (even though some overlaps might occur). To avoid overlapping, an expected value should be used if the distribution of data set is normal; if it is not the case a median or mean estimated by a 'Maximum-likelihood' method is recommended. Autocorrelation or rather a planar correlogram is suitable for analyzing planar continuity in three-dimensions. The functional relationship between the semivariogram (of at least the second order stationary regionalized variable) and its planar autocorrelation allow the autocorrelogram surface to be used as a spatial continuity of the original data. Thus the planar autocorrelogram gives the complete geostatistical system of the measured data. The Laplacian operator is a mathematical tool used for determining the net recharge and discharge volume for a physical quantity at a given point. Grid contours generated with the operator coincide with the structural and heterogeneity characteristics of clastic sedimentary rocks and thus the method is suitable for to indicating potential static flow surfaces or paths. Adoption of this method in coreflood experiments improves — on a micro scale — the comprehension and predictability of fluid motions in reservoir beds. This paper has two main goals: first, is to show that basic clastic sediments and sedimentary rocks are numerically identifiable and clearly distinguishable from each other on the basis of CT derived data analysis. The second goal to demonstrate that grid contours generated with the Laplacian operator coincide with the structural characteristics and inner heterogeneity of sedimentary rocks; and the method is suitable for indicating the potential flow surfaces or paths of clastic sedimentary rocks within the range of resolution of medical CT.

Introduction

Computerized X-ray tomography has been applied in geosciences for a considerable period of time. This non-destructive technique is adequate for investigating of the internal structure of various categories of volcanic, metamorphic, and sedimentary rocks. Sedimentary rocks are classified as nonsiliciclastic and siliciclastic depending on the origin of the constituents. Siliciclastic rocks are composed predominantly of terrigenous constituents derived from subaerial weathering processes and volcanic activity.

HONARPOUR et al. (1985) showed the functions of X-ray beam attenuation when crystalline solids were scanned. X-ray attenuation value varies with the size of the mineral, the orientation of the X-ray beam with respect to the crystallographic axes, the quality of the crystals, mineral orientation in the rock fabric, and the microscopic heterogeneity of the fabric due to reorientations and recrystallizations during lithification.

Another application of CT scanning is with the using of digital images to describe facies in terms of sedimentary transport processes and climatic variations. ROSS (1993) used CT to recognize coastal sediment transport processes, while LONG & ROSS (1991) applied it to identify depositional systems and deltaic evolution. Many studies investigate bed thickness in order to determine the variability of sediment rate (e.g. AGTERBERG & BANERJEE 1969; BESRÉ and OCCHIETTI 1990). By obtaining data along the longitudinal axe of a core sample a density series can be constructed. Such a series represents the geologic time and deposition, and contains information about the physical properties of the sediment at a given level. By plotting density data on an equidistant scale we get a time-sequence. Time-

sequence analysis can reveal the cyclical character of deposition, taking resolution of medical CT into consideration (HUNYADFALVI 2004).

X-ray attenuation coefficients recorded as raw CT data are the basis of the numeric or quantitative analysis of samples (KENTER 1989; KAWAMURA 1990; CARLSON & DENISON 1992; KANTZAS et al. 1992; FÖLDES 1993; BOSSCHER 1993; ORSI et al. 1994; BOESPFLUG et al. 1995; DENISON et al. 1997; FÖLDES et al. 2000; VANDERSTEEN et al. 2003; HUNYADFALVI 2004). Furthermore, numeric analysis proved to be efficient in revealing features that would otherwise be hardly visible.

CROMWELL et al. (1984) stated that non-destructive CT scanning would aid petroleum industries by imaging fluid flow in porous media. Petroleum engineers use CT data to study two-fluid coreflood experiments in reservoir lithologies (WELLINGTON & VINEGAR 1987; WITHJACK 1987), and to evaluate physical properties such as porosity and density (WELLINGTON & VINEGAR 1987; KANTZAS et al. 1992; ORSI et al. 1994; FÖLDES et al. 2004). Coreflood experiments are important in determining the index number for rock fluid interaction (that is, relative permeability): the visual displaying of the changing dynamism of saturation distribution also improves the comprehension and predictability of fluid motions in reservoir beds.

Many studies have investigated the role of CT scanning in single or multiple-phase processes (but these will not to discussed here in detail).

This paper has two main goals: first, is to show that basic clastic sediments and sedimentary rocks are numerically identifiable and clearly distinguishable from each other on the basis of CT-derived data analysis; the second is to demonstrate that grid contours generated with the Laplacian operator coincide with the structural characteristics and inner heterogeneity of sedimentary rocks and, furthermore, the method is suitable for indicating the potential flow surfaces or paths of clastic sedimentary rocks within the range of resolution of medical CT.

Principles of CT

X-ray computer tomography is based on the attenuation of X- or gamma rays emitted from an X-ray tube. Gamma rays interact with the matter in four ways: Raleigh scattering, photoelectric effect, Compton Effect, and pair generation (SIEGBAHN 1965). All these interactions depend on photon energy and the atomic number of the matter. A thin, well-collimated beam of X-ray attenuates following Beer's law:

$$I = I_0 exp\ (-\mu x)$$

where I_0 is the integral current of incident X (gamma) photons; I is the integral current transmitted by the sample; μ is the linear attenuation coefficient of the sample; and x is the sample width.

Three of the four interacting effects (Raleigh scattering, photoelectric and Compton effects) occur between 30 and 200 keV, which is the operating range of the most modern CTs. In cases in which there is a predominance of the Compton effect (above 100keV), the μ depends only on the density of the sample and not on its chemical composition. This is the case for most of the present day medical CTs. On the other hand, when the photoelectric effect dominates, the μ coefficient depends

also on the chemical composition of the absorbent. For samples which are not homogeneous, like clastic sedimentary rocks, the attenuation coefficient has different values at different points of the sample. This is why the linear attenuation coefficient μ depends on both the effective atomic number and the density of the object (CURRY et al. 1990).

At the end of the CT image reconstruction process, the result is a numerical map consisting of all the attenuation coefficients corresponding to each volume element (voxel). The values expressed as non-dimensional CT number (Hounsfield Units or HUs), according to the following relation:

$$HU = \frac{(\mu - \mu_{water})}{\mu_{water}} \times 1000 \ .$$

The fixed values of this scale take –1000 for the air and 0 for the water. The greater is the value of μ, the higher is the corresponding HU. The degree of attenuation is conventionally expressed in Hounsfield Units normalized by the attenuation coefficient of pure water (see KAWAMURA 1990; COLLETTA et al. 1991; FÖLDES 1993; INZAKI et al. 1995; OHTANI et al. 2000).

Reconstructed CT images are usually displayed as negative images where lighter tones represent higher HU values and, in contrast, lower HU values correspond to darker regions of the image. The difference between these regions is relative and thus there is no "uniform" scale to which reference can be made. Every core sample is a different case study: furthermore, there are certain conditions that need to be taken into consideration and these are dealt with in the next section.

The average 0.3–0.4 mm resolution of medical CT is not suitable for detecting mineral grains, for direct investigation of pore space, or for measuring the size of the pore throats. On the other hand, it is quite suitable as a macro-scale which can detect changes in the texture/fabric of sedimentary rocks linked to the changes of the character of deposition. Prior to this observation GEIGER et al. (2007) proved the significant genetic connection between the vertical sedimentary sequences which represent the depositional character of sedimentary facies and the correspondent rock density profiles.

Some mathematical calculations cannot be carried out on the set of non-positive numbers; therefore Hounsfield Units should be corrected with +1024 prior to any numerical evaluation. This 1024 must be extracted before calculation of CT numbers (CTN) (see details below).

Basic sedimentological principles

From the difference between the depositional environment and the depositional conditions, by definition (MOLNÁR & GEIGER 1981) it follows that any depositional environment consists of the system of depositional conditions and their rock equivalents (GEIGER 1986). The vertical succession of the individual facies of some depositional environments — e.g.: a point-bar, a channel or the natural levee of a fluvial environment — does not necessarily mean that the rock types have been changed. On the other hand, it is true that the temporal constancy of some

depositional environment resulted in concordant bedding of different rocks due to changeability of sedimentary processes. Thus it cannot be accepted that the extension of the term sedimentary bed follows for every bounding surface which reflects the regional change of the depositional process (MAJOROS 1966, p. 5; cited after GEIGER 1986). This statement is not a rejection of the descriptive character of the sedimentary bed. In the case of clastic sedimentary rocks the use of term 'bed' as a rock type is inappropriate in a genetic sense because it does not fulfil the genetic aspect of the reconstructionm of the environment. Consequently, 'sedimentology depositional facies' refers to the vertical succession of rocks that are in a genetic relationship.

Different Hounsfield Units, with respect to the different rock types of different ages, help to identify alterations in the sedimentary texture/fabric and bulk density. However, different attenuation coefficient values may correspond to rocks of equivalent grain size but of different degrees of diagenesis. The characteristic properties of clastic sedimentary rocks reflect the general effect of the various physical, chemical and biological processes. Synsedimentary and post-sedimentary processes, diagenesis, primary and secondary porosity and geological time play primary roles in affecting the texture, fabric, and bulk density of sedimentary rocks. Consequently, quantitative comparisons can involve samples from almost similar depositional environments with slight differences in the degree of diagenesis.

Tools and samples

CT measurements have been carried out at the Institute of Diagnostic Imaging and Radiation Oncology, University of Kaposvár, where a Siemens Somatom Plus 40 instrument was used. The slice thickness is 2 mm; the pixel size is 0.33×0.33 mm, and the measurements were made for a single slice. The original image consisted of 512×512 voxels and thus the field of view (FOV) was 512×0.33 mm — that is approximately 16.98 cm. The highest resolution of the Somatom Plus 40 is 0.1×0.1×1 mm. The instrument operates at 140 kV, with a 189 mA current, and 1.5 s exposure.

Core samples analyzed are from the collection of the Department of Geology and Palaeontology, University of Szeged, and Mol (Hungarian Oil and Gas Co.). The collection contains samples from the Pannonian Basin filled with sediments which came from a delta-fed turbidity fan, of Pannonian age (Pannonian *sensu lato* 12.6–2.4 Ma). The fan morphologically fits in with the Walker-type fan model (WALKER 1978), and satisfies the criteria of a point source mud/sand-rich submarine fan (READING & RICHARDS 1994).

The main reason for choosing samples is so that they have characteristic and easily identifiable textural, structural features, visible to the naked eye.

Methods

The measurement provides attenuation coefficient values arranged in a 512×512-size grid. Each grid is easily visualized by using any surface modelling system, like Surfer 8, a product of Golden Software. To avoid data-lossthe 'Nearest neighbour' method should be used to calculate grid contours, and define grid

spacing as one in both X and Y directions. Thusit is possible to visualize the real CT data, and the image has a better resolution. Among the several advantages of this solution, the most important ones are: (1) the grid/extract command in Surfer 8.0 creates a subset of an existing grid file to focus on some important data geometry at the so-called data-level. (2) the grid/blank command removes grid node data from a grid in areas where it is not desired to display contours on a map, and data of the blanked grid can be easily exported to any statistical programs (in this paper SPSS 11.0, and Statgraphics 3.0 were used). (3) the grid representation is appropriate for studying the spatial continuity of HU values (e.g. by counting the grid correlogram), or to search for some repetitive pattern by computing the grid periodogram; (4) this solution provides a direct way of connecting the data-preparation, the mathematical-statistical analyses, and the spatial analyses phases.

Every type of texture could be represented by an interval of HU values. The problem is that sometimes these intervals overlap so it is difficult to distinguish them explicitly in a numerical way. To overcome the problem in the numerical identification of the basic clastic sedimentary rocks two sample comparisons must be used in which the programme runs a Mann-Whitney W test to compare the medians of the two samples. This test is constructed by combining the two medians and the respective mean values of the data sets are then compared. Due to the non-normal distribution of sets coming from an irregular shaped grid, the contours of the mean of each data set are calculated using a 'Maximum-likelihood' method that is independent of the distribution type and robust with regard to the still existing extreme values. If the difference of two medians is less than 20 HUs — which is double the measuring noise of medical CT — the sets can be considered to be numerically equal. The choise of an interval (20 HUs) was considered necessary because data sets are obtained from different sizes of core samples and grid contours.

All statistical comparisons must follow sedimentological analysis in order to reveal the facies and the nature of the accumulation within depositional environments, since different facies of depositional environments create different textures and fabrics of clastic sedimentary rocks.

Linear geostatistics uses semivariograms to analyze the planar and spatial continuity of the regionalized variables. Autocorrelation or more precisely the planar correlogram is suitable for analyzing the planar continuity of slices perpendicular to the longitudinal axis of core samples. Anisotropy analysis on these grid contours is applicable because no interpretation between grid nodes was applied in order to generate the contours. There is a functional relationship between the semivariogram of at least a second order stationary-regionalized variable and its planar autocorrelation. The semivariogram surface can be obtained from the correlogram applying this theorem (GEIGER 2005). It is reasonable that the autocorrelogram surface that counts for the grid contour shows the spatial continuity of the original data. Consequently the planar autocorrelogram gives the complete geostatistical system of the measured values.

The determination of the static potential flow paths of the sedimentary rocks requires the application of the Laplacian operator. With the aid of the operator recharge and discharge areas and their surfaces can be identified easily. The Laplacian operator ($\partial^2 Z$) is a mathematical tool for determining the net recharge ($\partial^2 Z>0$) and

discharge ($\partial^2 Z<0$) volume for a given surface or rock volume. On the grid generated with the operator the recharge areas have positive signs while the discharge areas are negative. The flux of traditional physical quantities — like ground water, heat or electric charge — at a given point is the function of the gradient of that point. The determination of the gradient is possible with the following equation:

$$\partial^2 Z = \frac{\delta^2 z}{\delta x^2} + \frac{\delta^2 Z}{\delta y^2}.$$

Results

The value of X-ray attenuation usually depends generally on bulk density, effective atomic number, fluid content,the chemical composition of the grains, cement and fluid if present in clastic sedimentary rocks (HUNT et al. 1988; KNOLL 1989; BOESPFLUG et al. 1995).

The debris materials of Pannonian sediments consist of metamorphic and quartz gravels; the cements are dark grey siltstone, clay, light grey carbonate containing siltstone and sandstone (BÉRCZI & VICZIÁN 1973). Most of the samples are quartzose litharenite, litharenite and feldspathic arkose (*Figure 1*). Core samples from the Algyő region include sandstone ripples, dunes and massive sandstone beds, in alternation with siltstone and argillaceous marl beds. The mean values of the sandstone beds (regardless of their mineral content) from the A–248/1, A–248/2 and A–100 boreholes were 2604, 2718, and 2663 HUs, respectively.

The CTN or CT numbers, proposed by AMOS et al. (1996) were derived from HUs as follows:

$$CTN = \frac{HU}{1000} + 1.$$

The main benefit of CTN over HUs is that they give a better approach to sample densities expressed in the traditional gr/cm^3 form. The CT numbers for the same samples analyzed are 2.58, 2.69 and 2.64, respectively. These values are within the statistical error limit of the density of the quartz mineral which is 2.65 gr/cm^3. Note that 1024 must be extracted from Hounsfield Units before applying the equation.

Grain size is an important factor which effects X-ray attenuation. The resolution of medical CT is suitable for detecting changes in X-ray attenuation

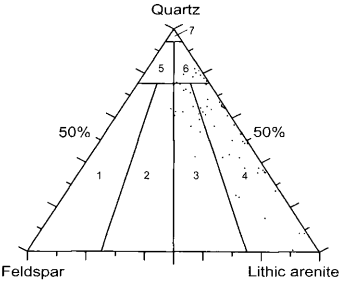

Figure 1. Mineral content of sediments of the conglomerate level with Lower-Pannonian age. Legend: 1 arkose, 2 litharenitic arkose, 3 feldspathic arkose, 4 litharenite, 5 quartzose arkose, 6 quartzos litharenite, 7 quartzite. After BÉRCZI & VICZIÁN (1973)

1. ábra. Az alsó-pannóniai konglomerátum szint üledékeinek ásványos összetétele. Jelmagyarázat: 1. arkóza, 2. „kőzethomokos" arkóza, 3. földpátos kőzethomok, 4. kőzethomok (litoarenit), 5. kvarcos arkóza, 6. kvarcos kőzethomok, 7. kvarcit. Átdolgozva BÉRCZI & VICZIÁN (1973) nyomán

which have their origins in grain size alteration above 0.1 mm. Sedimentary rocks with a smaller mean grain size have higher X-ray attenuation than rocks with a bigger mean grain size with regard to slight differences in age and depositional history (*Figure 2*) (HUNYADFALVI 2006). Compaction and cementation are processes that increase bulk density and decrease porosity. The higher degree of the diagenetic stage means a greater bulk density, tighter packing, higher X-ray attenuation and higher Hounsfield

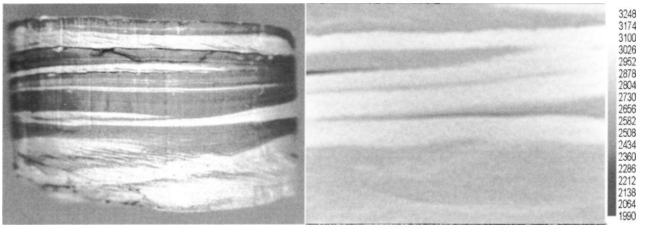

Figure 2. Fine sandstone and siltstone with the same depositional origin and age. These rocks represented by different X-ray attenuation coefficients due to different mean grain sizes. On the right is the grid contour of Hounsfield Unit (HU) values. Higher HU values (light grey) represent smaller mean grain size

2. ábra. Hasonló felhalmozódási eredetű és korú finomszemű homokkő és aleurolit. Az eltérő szemcseméretből adódóan, különböző röntgensugárzás gyengítési együtthatóval jellemezhetőek. A jobb oldali képen a Hounsfield egységek (HE) grid kontúrja látható. A nagyobb HE értékek (világos szürke), kisebb szemcseméretet jelölnek

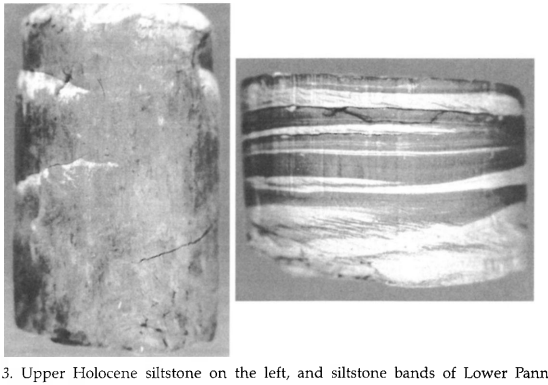

Figure 3. Upper Holocene siltstone on the left, and siltstone bands of Lower Pannonian siltstone on the right (dark grey bands). They represent two different diagenetic stages; therefore, the Hounsfield units concerning to them are also different

3. ábra. Felső-holocén aleurolit (bal oldali kép), valamint alsó-pannóniai aleurolit (sötétszürke sávok) és homokkő (jobb oldali kép). A minták, két eltérő diagenizáltsági állapotot reprezentálnak, ebből kifolyólag, a HE értékek is különbözőek

Units. Generally, older rocks represent higher diagenetic stages and therefore bulk density values (rather than younger rocks) so they are represented by higher Hounsfield Units. On *Figure 3* there are two siltstones representing two diagenetic stages due to different geological ages. On the left hand photo there is an Upper Holocene siltstone with (median 2193 HUs) (HUNYADFALVI 2004), while the other one on the right is with a Lower Pannonian siltstone (median 2869 HUs). The main difference between them is the degree of the diagenetic stage they are at.

Basic clastic sediments and sedimentary rocks are numerically identifiable and can easily be distinguished from each other on the basis of CT-derived data analysis taking age and depositional history into consideration. 13 core samples involved in the numerical comparison were subdivided into coarse grain-size sets and fine grain-size sets. The boundary between coarse and fine sediments is 0.0625 mm or $\Phi = 4$. The Φ corresponds to the diameter of the particles according to the equation: $\Phi = -\log_2 d$ (KRUMBEIN & SLOSS 1963), where d is the diameter in millimetres. Prior to statistical comparison outlier and extreme data must be removed from sets of coarse and fine grain size data sets, respectively, using the Box-Whisker plot technique. This step ensures that only appropriate data are taken into consideration. All coarse grain-size sets have to be compared to each other in order to reveal numerical identity or difference between them (*Figure 4*). The same procedure is carried with fine grain size

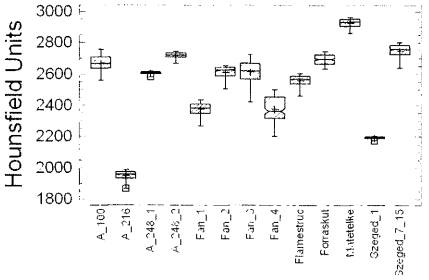

Figure 4. Coarse grain size sets are compared to each other to reveal numerical identity. Two sample comparisons run a Mann-Whitney W test to compare the medians of the two samples

4. ábra. A durva szemcseméretű adathalmazok összehasonlítása, feltárja az esetleges numerikus azonosságokat. Az eljárás során a mediánok páronként, a Mann-Whitney-féle W teszt alapján lettek összehasonlítva

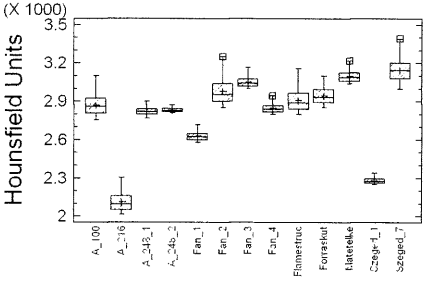

Figure 5. Fine grain size sets are compared to each other to reveal numerical identity. Two sample comparisons run a Mann-Whitney W test to compare the medians of the two samples

5. ábra. A finom szemcseméretű adathalmazok összehasonlítása. Az eljárás során a mediánok páronként, a Mann-Whitney-féle W teszt alapján lettek összehasonlítva

sets either (*Figure 5*). Results show that data sets are statistically different from each other on the basis of their medians and means. On *Figure 4* and *Figure 5* the data sets of core samples are displayed in one graph in order to reveal significant numerical difference or lack of difference between the median values. There are five data pairs from the coarse grain-size sets whose medians are within the 20 HU-interval, so they seem to be numerically identical (*Figure 6*). Sedimentological analysis verifies this assumption: the sandstones of numerically identical data pairs are from the same

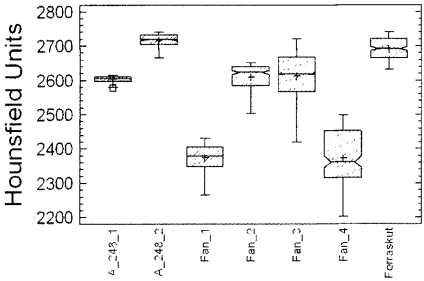

Figure 6. There are five pairs of samples: A–248/1–Fan/3, A–248/1–Fan/2, A–248/2–Forráskút, Fan/1–Fan/4, and Fan/2–Fan/3 that are numerically identical on the basis of their medians

6. ábra. A mediánok alapján öt adathalmaz-pár numerikusan azonosnak mutatkozott

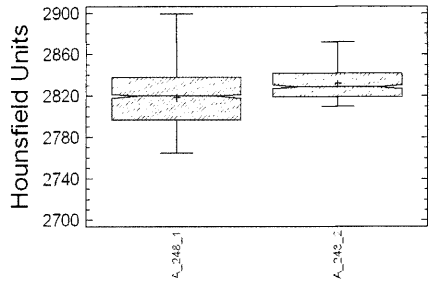

Figure 7. These two core samples are numerically identical based on two sample comparison of median values of the fine grain size sets

7. ábra. A finom szemcsemérethez tartozó adathalmazok mediánjai egymástól numerikusan nem különböztethetőek meg

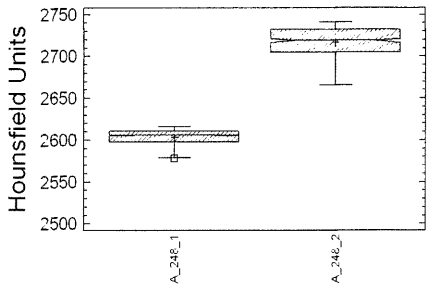

Figure 8. The same core samples proved to be numerically different based on two sample comparison of median values of the coarse grain size sets

8. ábra. Ugyanazon fúrómagok durva szemcseméretihez tartozó adathalmazainak mediánjai numerikusan különbözőek

depositional environment (i.e. the distributary channel deposits of a submarine fan) with similar accumulation conditions.

There are two samples from the same borehole with a few tens of centimetres of vertical separation that are numerically identical on the basis of the respective medians of fine grain size sets (*Figure 7*), and different on the basis of the medians of coarse grain-size sets (*Figure 8*). These statements seem to contradict to each other. Basically, fine grains are not involved in traditional statistical grain size analysis, because grains finer than fine sand could have been deposited by different agents

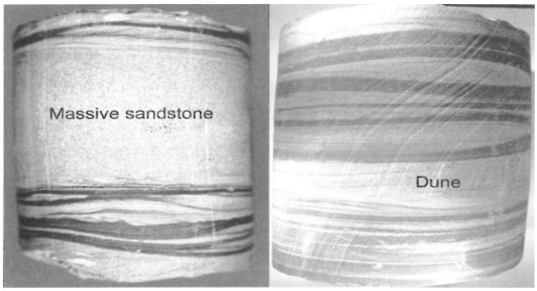

Figure 9. Two core samples from the same borehole with a few of tens of centimetres vertical separation from each other. There is massive sandstone in the middle of core sample on the left (A–248/1). On the right, there are dune and ripple sands (A–248/2). Different textural characteristics are the basis of different median values of Hounsfield Unit values

9. ábra. Ugyanazon fúrásból származó magminták, néhány tíz centiméter függőleges távolságban egymástól. A bal oldali ábrán látható minta (A–248/1) középső részén szerkezet nélküli homokkő látható. A jobb oldali minta (A–248/2) homokdűnékből, homok fodrokból áll. Az eltérő szöveti (texture) tulajdonságoknak, eltérő HE értékek a következményei

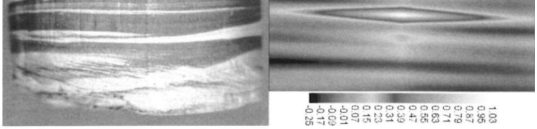

Figure 10. Photo and correlogram of core sample A-100. The anisotropy ellipse shows near horizontal continuity. The alteration of light and dark grey bands represents zonal anisotropy that coincides with the structure of core sample

10. ábra. Az A–100 jelű minta fotója és korrelogramja. Az anizotrópia ellipszis közel vízszintes folytonosságot jelöl. A világosabb és sötétebb szürke sávok váltakozása zonális anizotrópiát mutat, amely megegyezik a mintán látható szerkezettel

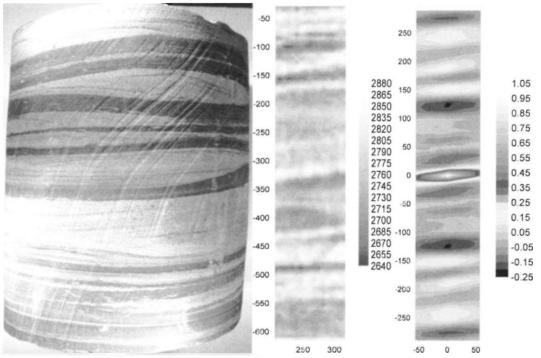

Figure 11. Zonal anisotropy of core sample A–248/2 derived from horizontal and wavy bedding of alternating silty and sandy sediments. Grid contour (in the middle) is narrower than the real sample in order to deal with unbiased data only

11. ábra. Az A–248/2 jelű mintán szintén zonális anizotrópia figyelhető meg; oka a horizontális, hullámos rétegzettségű homokkő és aleurolit váltakozása. A középső ábrán látható grid kontúr keskenyebb, mint a minta annak érdekében, hogy a számítási műveletek csakis a valós adatokkal valósuljanak meg

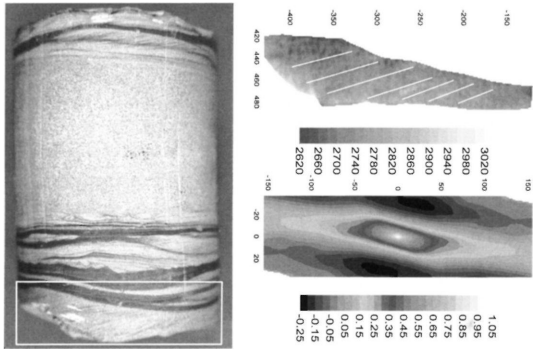

Figure 12. There is a dune form on the lowermost part of the sample (white rectangle). Laminae are also visible on the grid contour indicated by white lines (upper right). Autocorrelogram shows an elongated inner heterogeneity originated in downstream migration of the dune

12. ábra. A minta alsó részén dűneforma látható (fehér négyszög). A jobb felső ábrán látható grid-kontúron jól láthatóak a dűnét felépítő réteglemezek (fehér vonalakkal kiemelve). Alatta az autokorrelogramon elnyújtott, enyhén ívelő főtengelyű anizotrópia ellipszis figyelhető meg. Ez nagyon jól egybevág a dűneforma folyásirányba történő migrációja miatt kialakuló belső heterogenitási iránnyal

and the difference between the character of the agents cannot be revealed due to the lack of any significant mark indicating the way of transportation as identified on the grains. The sandstone from core sample A–248/1 is of a massive nature with abrupt, fall-like accumulation caused by the turbidity current. On the other hand, the sandstone from core sample A–248/2 is dune and ripple sand; it has graded bedding laminae due to the lower flow velocity and traction carpet sedimentation (*Figure 9*). The difference in texture also means there are differences in the respective median values of the Hounsfield Units.

The spatial continuity and anisotropy of grid contours reflect the original texture and structure relations of the core samples. On *Figure 10*, the correlogram of core sample A–100 coincides with the structure of the sample, and reveals zonal anisotropy which had its origins in the vertical alteration of the sandstone and siltstone beds. In other words, the longer axis of the anisotropy ellipse is nearly horizontal, as is indicated by the layer boundaries. Zonal anisotropy is also visible on the correlogram of core sample A–248/2 (*Figure 11*). The grid contour and correlogram of sample A–248/2 is narrower than the original core sample due to the extraction of inappropriate data in order to use real HU values which only correspond to each of the rock types.

There is a dune form on the lowermost part of sample A–248/1 and its spatial heterogeneity is linked to its genetics (*Figure 12*). Laminae are visible on the grid contour and the anisotropy grid shows a rather elongated form derived from dune downstream migration.

The amalgamation surface is a planar fabric across which two turbidity bodies are joined (MATTERN 2002). Its horizontal continuity — represented by the correlogram generated from the grid contour (*Figure 13*) — verifies the genetics of the surface.

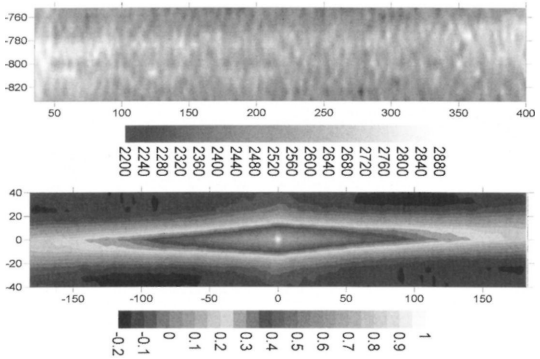

Figure 13. The grid contour (upper) and the correlogram (lower) of amalgamation surface. Anisotropy ellipse indicates the near horizontal continuity that is derived from its genetics

13. ábra. Az összeolvadási felszín grid kontúrja (felső) és autokorrelogramja (alsó). Az anizotrópia ellipszis, közel horizontális folytonossági irányt jelöl, amely az összeolvadási felszín kialakulására vezethető vissza

Zones of weakness or potential flow paths can be easily identified on grids generated with the Laplacian operator. In core sample A–100 the lower bounding planes of the sandstones which are erosional surfaces are the recharge areas where the least resistance occurs (*Figure 14*). The same features can be seen on core sample A–248/2 (*Figure 15*). Both samples are typical instances of the horizontal bedding of silty and sandy sediments, where erosive surfaces were generated by higher energy currents. The autocorrelogram of the amalgamation surface shows horizontal

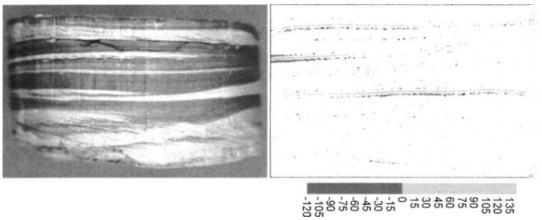

Figure 14. In core sample A–100 the potential flow paths are highlighted by erosional surfaces that represent the lower bounding planes of sandstones. Values above zero indicate recharge areas (light grey)

14. ábra. Az A–100 jelű mintában a potenciális áramlási pályákat, a homokköveket alulról határoló eróziós felszínek jelölik ki. A grid-kontúron a nullánál nagyobb, világosszürke adatpontok az összeáramlási zónákat jelölik

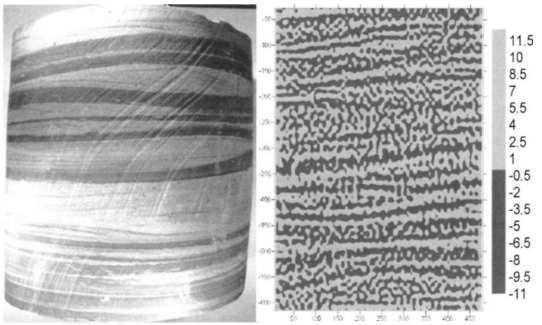

Figure 15. As seen on Figure 14 bounding planes of alternating siltstone and sandstone beds indicate sharp potential flow paths since they represent the paths where the least resistance occurs

15. ábra. A 14. ábrához hasonlóan, az A–248/2 mintán is a homokköveket alulról határoló eróziós felszínek képezhetik az áramlás lehetséges útvonalát, hiszen ezek a legkisebb ellenállású zónák

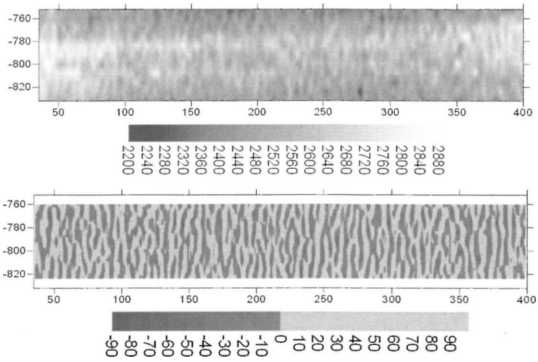

Figure 16. Potential flow paths of amalgamation surface (lower) show vertical orientation in contrast with anisotropy ellipse see on Figure 13. It could be due to abrupt accumulation governed by gravity

16. ábra. Az összeolvadási felszín potenciális áramlási pályái függőleges orientációt mutatnak (alsó), amely ellentétben áll a 13. ábrán látható anizotrópia-ellipszis által kijelölt fő folytonossági iránnyal. Ennek oka a gravitáció hatására bekövetkezett gyors akkumuláció lehet

continuity (*Figure 13*). In contrast to this the potential flow paths seem to be vertical, being derived from the abrupt, fall-like accumulation of the sediments (*Figure 16*). Core flood experiments are needed to reveal the inner heterogeneity of these surfaces and accept or reject the assumptions.

Discussion

The core samples analyzed some 34 years ago by BÉRCZI & VICZIÁN (1973) represent a more than three-decade-old method for mineral content analysis. It means the results the scientists acquired then could be different now with application of state-of-the-art methods. Unfortunately, the author did not have the possibility to accomplish any mineral content analysis, so he was constrained to accept the formerly calculated results. The fact that the CT numbers are within the statistical error limit of the density of the quartz mineral (2.65 gr/cm^3) shows that CT measurements give reasonable enough results with respect to the dominant mineral component of sandstones with Early Pannonian age and which affect X-ray attenuation. Due to the resolution of medical CT information can be gained about the 2 mm^2 area times the thickness of the slice (known as voxel, the pixel in 3D) of the core sample (which is too big to decide the affect of each mineral grain on X-ray attenuation). The mineral composition varies randomly from voxel to voxel and there is no correlation between the respective compositions of neighbouring voxels. Thus, there is no chance to generate a "uniform" scale to which data can be assigned.

Diagenesis is the collective term for several physical, chemical and biological processes that affect the physical and chemical properties of sedimentary rocks. The mineral content, pressure, temperature, the character and flux of pore filling fluids, porosity, and permeability all have an influence on the processes taking place during lithification and diagenesis. Due to the complexity of the diagenetic processes it is a difficult task to emphasize with certainty the dominance of one or two of them which having the largest effect on the bulk density and X-ray attenuation.

The resolution of the medical CT is unsuitable for detecting single grains, pores or for the indirect determination of the size of pore throats. Although, this is true, the former statement concerning the relationship between grain size and the attenuation coefficient — i.e. the smaller the grain size, the higher the attenuation coefficient — also has some truth. Two basic sedimentary rock types from the same depositional environment, with the same age and diagenetic stage represent two different medians, expected values or means of CT data sets. The main difference between them is the type of accumulation. Finer sediments tend to accumulate during low velocity; the packing is tighter and therefore the bulk density is higher, so is the attenuation coefficient or Hounsfield Unit, regardless of the mineral content.

Conclusions

Medical CT measurements provide reasonable enough data to enable the application of numerical analysis in order to identify and distinguish basic clastic sedimentary rock types, taking age and depositional history into consideration. X-ray attenuation of clastic sedimentary rocks generally depends on the bulk density, effective atomic number, fluid content, and chemical composition of the grains, cement, and fluid content (if present). Supposing that age and the nature of deposition are nearly the same, a smaller mean grain size indicates higher X-ray attenuation due to tighter packing and higher bulk density.

The mineral composition of clastic sediments vary randomly from voxel to voxel in the 3D matrix and therefore it should not be over-emphasized as a significant factor affecting X-ray attenuation, since the resolution of medical CT is inappropriate for detecting individual grains.

The resolution of medical CT is suitable for detecting changes in texture and fabric which have their origins in grain size fluctuation derived from fluctuation of agent velocity and the type of deposition. Every type of texture/fabric could be described by intervals of Hounsfield Units. To avoid overlapping numerical identification adopts two sample comparisons in which medians of the data are compared. Medians of data should be used when distribution of the data are non-normal. In the case of non-normal distribution the use of mean value, estimated by a "Maximum-likelihood" method, is also feasible. Sedimentological investigation must follow every numerical comparison in order to verify or reject mathematical assumptions concerning the differences between the data sets that are being compared.

Utilization of the functional relationship between the semivariogram of at least a second order stationary regionalized variable and its planar autocorrelation is essential in order to reveal micro-scale spatial continuity of clastic sedimentary rocks. Results have proved that autocorrelograms give appropriate images of spatial continuity or zonal anisotropy.

The potential that lies in the application of the Laplacian operator is promising with respect to indicating small-scale static flow surfaces. These surfaces or zones are linked to erosional surfaces, layer boundaries, or any fabric-controlled regions that are less coherent in the field of clastic sedimentary rocks deposited in a submarine fan environment. Detection of such zones based on data obtained from CT measurements could be revolutionary in micro-sedimentology, and further developments could aid petroleum geology.

Acknowledgements

The author wish to thank the following for their contributions to the completion of this paper: Tamás FÖLDES, Institute of Diagnostic Imaging and Radiation Oncology, University of Kaposvár; Dr. János GEIGER, associate professor, Department of Geology and Palaeontology, University of Szeged; Dr. Péter Bogner, director, Institute of Diagnostic Imaging and Radiation Oncology, University of Kaposvár.

References — Irodalom

AGTERBERG, F. P. & BARENJEE, I. 1969: Stochastic model for the deposition of varves in glacial lake Barlow-Ojibway, Ontario, Canada. — *Can. J. Earth Sci.* **6**, 625–652.

AMOS, C. L., SUTHERLAND, T. F., RADZIJEWSKI, B. & DOUCETTE, M. 1996: A rapid technique to determine bulk density of fine-grained sediments by X-ray computed tomography. — *J. Sediment. Res.* **66**, 1023–1024.

BESRÉ, F. & OCCHIETTI, S. 1990: Les varves de Deschaillons, les rhythmites du saint-Maurice et les rhythmites de Leclercville, Pleistocéne supérieur, vallée du Saint-Laurent, Québec. — *Géogr. Phys. Quat.* **44/2**, pp.181–198.

BÉRCZI, I. & VICZIÁN, I. 1973: Sedimentological analysis of Neogene sediments in the Southern Great Plain, Hungary. — *Földtani Közlöny* **103**, 319–339.

BOESPFLUG, X., LONG, B. & OCCHIETTI, S. 1995: CAT-scan in marine stratigraphy: a quantitative approach. — *Marine Geology* **122**, 281–301.

BOSSCHER, H. 1993: Computerized tomography and skeletal density of coral skeleton. — *Coral Reef* **12**, 97–103.

CARLSON, W. D. & DENISON, C. 1992: Mechanism of porphyroblast crystallization: results from high resolution computed X-ray tomography. — *Science* **257**, 1236–1239.

COLLETTA, B., LETOUZEY, J., PINEDO, R., BALLARD, J. F. & BALÉ, P. 1991: Computerized X-ray tomography analysis of sandbox models: examples of thin-skinned thrust systems. — *Geology* **19**, 1063–1067.

CROMWELL V., KORTUM, D. J. & BRADLEY, D. J. 1984: The use of a medical computer tomography (CT) system to observe multiphase flow in porous media. — *Soc. of Petroleum Eng.* Richardson, TX: 13098

CURRY, T. S., DOWDEY, J. E. & MURRY, R. C. Jr. 1990: Christensen's Physiscs of Diagnostic Radiology. — 4th edition Lea and Febiger, Philadelphia, 376 p.

DENISON, C., CARLSON, W. D. & KETCHAM, R. A. 1997: Tree-dimensional quantitative textural analysis of metamorphic rocks using high resolution computed X-ray tomography: Part I. Methods and techniques. — *Journal of Metamorphic Geology* **15/1**, 29–44.

FÖLDES, T. 1993: New interpretation methods of Diplog for recognition the internal structure of thereservoir. — Poster, OMBKE Conference, Tihany, Hungary

FÖLDES, T., KISS B., ÁRGYELÁN G., BOGNER, P. & REPA, I. 2000: Application of medical computer tomograph measurements in 3D reservoir characterization. — *EAGE SAID Conference, Paris, France*

FÖLDES, T., KISS, B., ÁRGYELÁN, G., BOGNER, P., REPA, I. & HIPS, K. 2004: Application of medical computer tomograph measurements in 3D reservoir characterization — *Acta Geologica Hungarica* **47/1**, 63–73.

GEIGER, J. 1986: Üledékes homokkőtestek szöveti és morfogenetikai vizsgálata. (A textural and morphogenetic study of sandstone bodies.) — *Földtani Közlöny* **116**, 249–266.

GEIGER, J. 2005: A CT vizsgálatok és a laboratóriumi kőzetfizikai vizsgálatok eredményeinek numerikus kiértékelése. (Numerical analysis of CT measurements and laboratory pertophysical investigations.) — *Kézirat*, 5 p.

GEIGER, J., HUNYADFALVI, Z. & BOGNER, P. 2007: Analysis of small-scale heterogeneity in clastic rocks by using computerized X-ray tomogrpahy (CT). — *Journal of Engineering Geology* (In print)

HONARPOUR, M. M., CROMWELL, V., HATTON, D. & SATCHWELL, R. 1985: Reservoir Rock Descriptions Using Computed Tomography (CT). — *Paper SPE 14272 presented at the Annual Technical Conference and Exhibition, Las Vegas, Sept. 22–25.*

HUNT, P. K., EUGIER, P. & BAJSAROWICZ, C. 1988: Computed tomography as a core analysis tool: applications, instrument evaluation, and image improvement techniques. — *Soc. Pet. Eng.* 1203–1210.

HUNYADFALVI, Z. 2004: Heterogeneity analysis of clastic sediments by computerized X-ray tomography. — *Acta Geologica Hungarica* **47/1**, 53–62.

HUNYADFALVI, Z. 2006: Small-scale heterogeneity analysis of clastic sediments by using X-ray computer tomography. — Ph. D. Thesis, Dep. Of Geology and Paleontology, University of Szeged, 19 p.

INZAKI, T., INOUCHI, Y. & NAKANO, T. 1995: Use of medical X-ray CT scanner for nondestructive and quantitative analysis of lake sediments. — *Bull. Geol. Surv. Japan* **46**, 629–642. (in Japanese with English abstract)

LONG, B. F. & ROSS, N. 1991: Études océonagraphiques physiques et biologiques: analyses compémentaires. — *Rapp. INRS-Océanol., Project SEBJ ILP–892–1–02*, 73 p.

KANTZAS, A., MARENTETTE D. F. & JHA K. N. 1992: Computer-assisted tomography: from qualitative visualization to quantitative core analysis. — *J. Canadian Petrol. Technol.* **31**, 48–56.

KAWAMURA, T. 1990: Nondestructive, three dimensional density measurements of ice core samples by X-ray computed tomography. — *J. Geophys. Res.* **95**, 12407–12412.

KENTER, J. A. M. 1989: Application of computerized tomography in sedimentology. — *Mar. Geotechnol.* 8, 201–211.

KNOLL, G. F. 1989: *Radiation detection and measurement.* — Wiley, New York, 30–102.

KRUMBEIN, W. C. & SLOSS, L. L. 1963: *Stratigraphy and sedimentation,* — San Francisco, Freeman, W. H., 96 p.

MATTERN, F. 2002: Amalgamation surfaces, bed thickness, and dish structures in sand-rich submarine fans: numeric differences in channelized and unchannelized deposits and their diagnostic value. — *Sedimentary Geology* **150**, 203–228.

MOLNÁR, B. & GEIGER, J. 1981: Homogénnek látszó rétegsorok tagolási lehetősége szedimentológiai, őslénytani és matematikai módszerek kombinált alkalmazásával. (Possible dismembering of seemingly homogeneous sequences by using sedimentological, paleontological and mathematical methods.) — *Földtani Közlöny* **111/2–3**, 238–250.

OHTANI, T., NAKASHIMA, Y. & MURAOKA, H. 2000: Three-dimensional miarolitic cavity distribution in the Kakkonda granite from borehole WD-1 using X-ray computerized tomography. — *Eng. Geol.* **56**, 1–9.

ORSI, T. H., EDWARDS, C. M. & ANDERSON, A. L. 1994: X-ray computed tomography: a nondestructive method for quantitative analysis of sediment cores. — *J. Sediment. Res.* **A64**, 690–693.

READING, H. G. & RICHARDS, M. 1994: Turbidite systems in deep-water basin margins classified by grain size and feeder system. — *AAPG Bulletin* **78/5**, 792–822.

ROSS, N. 1993: Les barres d'avant côte: géométrie des systémes, mécanisme de mise en place et concentration de minéraux lourds. — Ph. D. Thesis, Univ. Laval, Qué.

SIEGBAHN, K., 1965. Alpha-, Beta-, Gamma-ray spectroscopy. — North-Holland P. Co., Amsterdam. Vol 1. Chapters 5, 8A.

VANDERSTEEN, K., BUSSELEN, B., VAN DEN ABEELE, K. & CARMELIET, J. 2003: Quantitative characterization of fracture apertures using microfocus computed tomography. Applications of X-ray computed tomography in the geosciences. — *Geological Society Special Publications* **215**, 61–68.

WALKER, R. G. 1978: Deep-water sandstone facies and ancient submarine fans: Models for exploration for stratigraphic traps. — *AAPG Bulletin* **62/6**, 932–966.

WELLINGTON, S. L. & VINEGAR, H. J. 1987: X-ray computerized tomography. — *J. Pet. Technol.* **2**, 885–898.

WITHJACK, E. M. 1987: Computed tomography for rock-property determination and fluid-flow visualization. — *Soc. Pet. Eng.* **16951**, 183–196.

Kézirat beérkezett: 2007. 04. 16.